Scheme I. Reactions of Me_2NH with $M_3(CO)_9(\mu_3\text{-}S)_2$ Clusters

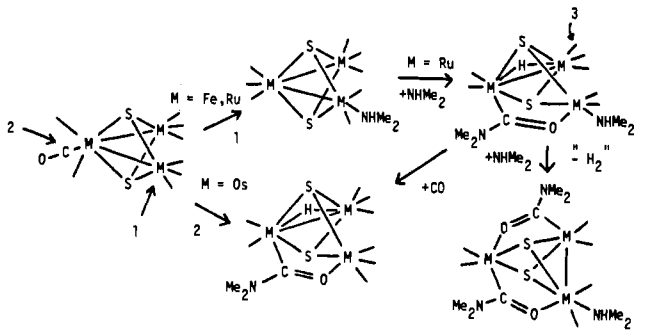

a rate that could be followed spectroscopically, and this has permitted the reaction sequence to be established. Before the formation of **2** occurred, an intermediate that was spectroscopically similar to $Fe_3(CO)_8(NHMe_2)(\mu_3\text{-}S)_2$ was formed. Accordingly, this intermediate has been formulated as **5** and this confirms that the first step in the formation of **2** is a CO substitution reaction on one of the two external metal atoms of cluster. See route 1 in Scheme I, which summarizes the reactions of all of the $M_3(CO)_9(\mu_3\text{-}S)_2$ clusters with Me_2NH. Only the osmium cluster reacts initially by route 2, which is attack upon a CO ligand in its first and only reaction step.

Unlike $Fe_3(CO)_8(NHMe_2)(\mu_3\text{-}S)_2$, **5** reacted with a second mole of Me_2NH by attack upon a CO ligand on the central metal atom of the cluster. This led to compound **2** by the formation of a bridging carbamoyl ligand. This reaction is believed to be analogous to the reaction of the sulfido–osmium cluster with Me_2NH. The mechanism of the shift of the hydrogen atom from the amine nitrogen atom to the cluster to become the bridging hydride ligand has not been established in these studies. Addition of CO to **2** yielded **4**, which would be the expected product from the addition of amine to CO ligand in **1**. We have not obtained any evidence for the formation of **4** by the latter route. The reason why **2** adds amine at a CO ligand and **1** does not is not clear, but the cleavage of the metal–metal bond could be an important factor. In the structure of $Fe_3(CO)_8(NHMe_2)(\mu_3\text{-}S)_2$, it was observed that the Fe–Fe bond, which included the amine-substituted iron atom, was much longer and, presumably, thus weaker than the other one. This is the bond that must be cleaved to form **2** from **5**, and if its cleavage has an important influence on the reaction rate, its weakening may produce a sufficient enhancement to permit the amine addition to proceed at a practical rate.

Compound **3** was formed from **2** by the addition of 1 equiv of Me_2NH. Attack is believed to occur at a CO ligand on the metal atom that contains three CO ligands (route 3). A second carbamoyl ligand is formed, and an equivalent of H_2 (not observed) must be eliminated. Mechanistically, it is believed that the hydride-bridged metal–metal bond is **2** is cleaved and the new carbamoyl ligand bridges that pair of metal atoms. As a consequence of the H_2 elimination a new metal–metal bond is formed, and all the metal atoms obey the 18-electron rule.

Acknowledgment. The research was supported by the National Science Foundation under Grant No. CHE-8416460. The AM-300 NMR spectrometer was purchased with funds from the National Science Foundation, Grant No. CHE-8411172.

Supplementary Material Available: Tables of anisotropic thermal parameters (U values) and hydrogen atom parameters (4 pages); tables of calculated and observed structure factors (34 pages). Ordering information is given on any current masthead page.

Contribution from the Departments of Chemistry, The Ohio State University, Columbus, Ohio 43210, and The University of Warwick, Coventry CV4 7AL, U.K.

Synthesis and Characterization of a Lacunar Bis(isothiocyanato)cobalt(III) Cyclidene Complex: A Structural Model for Distal Steric Effects in Hemoproteins

Patricia J. Jackson, Colin Cairns, Wang-kan Lin, Nathaniel W. Alcock,* and Daryle H. Busch*

Received February 12, 1986

The synthesis and structural characterization of lacunar bis(isothiocyanato)cobalt(III) cyclidene complexes are presented. The effect of the restrictive lacuna on axial ligation is clearly seen from the results of the X-ray crystal structure determination of one of the complexes. Bis(isothiocyanato)(2,3,9,10,12,18-hexamethyl-3,9,13,17,20,24-hexaazabicyclo[9.7.7]pentacosa-1,10,12,17,19,24-hexaene-κ^4N)cobalt(III) hexafluorophosphate crystallizes in the orthorhombic space group $P2_12_12_1$, with a = 10.342 (4) Å, b = 14.857 (4) Å, and c = 21.933 (4) Å, and was solved by the heavy-atom method to R = 4.2%, R_w = 4.7%. Both axial isothiocyanate ligands are appreciably bent as a result of very different steric influences. The ligand within the lacuna is distorted by intramolecular van der Waals interactions with the pentamethylene bridge, while that coordinated at the less hindered axial site bends because of an intermolecular interaction with a PF_6^- counterion in the crystal lattice. A comparison is made with the analogous hexamethylene-bridged cobalt(III) complex, in which the counterion is a chloride, and the various factors that may give rise to such distortions are discussed.

Introduction

It has been over 30 years since St. George and Pauling observed[1] that the sterically demanding binding site of hemoglobin results in reduced equilibrium binding constants for a series of alkyl isocyanides in the order $K_{EtNC} > K_{i\text{-}PrNC} > K_{t\text{-}BuNC}$. This seminal work has since been quantified in thermodynamic and kinetic studies of both natural heme proteins and model porphyrin systems, in attempts to rationalize the relative affinities for hemoproteins of carbon monoxide and dioxygen. Carbon monoxide binds in a linear fashion in virtually all its iron(II) porphyrin complexes, while dioxygen invariably adopts a bent end-on configuration.[2,3] In contrast, x-ray structural studies on carbon monoxide complexes of heme proteins show distortion from this ideal linear structure, but the nature of the distortion has been obscured by the limitations of the studies. It has been suggested that the natural hemoproteins discriminate against CO, and other linear diatomic ligands, via a steric interaction between the bound ligand and a "distal" amino acid side chain. In human hemoglobin the closest candidate for such an interaction is histidine-E7, although Val-E11

* Authors to whom correspondence should be addressed: N.W.A., The University of Warwick; D.H.B., The Ohio State University.

(1) St. George, R. C.; Pauling, L. *Science* (*Washington, D.C.*) **1951**, *114*, 629.
(2) Phillips, S. E. V.; Schoenborn, B. P. *Nature* (*London*) **1981**, *292*, 81.
(3) Shaanan, B. *Nature* (London) **1982**, *296*, 683.

0020-1669/86/1325-4015$01.50/0

and Phe-CD1 may also exert some influence.

The above observations have led several groups to design model porphyrin systems in an attempt to mimic the local environment of the hemoprotein binding site. Prominent among these are the picket-fence,[4] capped,[5] basket-handle,[6] and cyclophane[7] porphyrins, all of which provide a sterically hindered face at which small molecules may coordinate with varying degrees of difficulty. Most of these models have used amide linkages as a convenient synthetic means of attaching the desired bulky peripheral substituent. This leads to the possibility that the discrimination in binding constants involving dioxygen, carbon monoxide, and other small molecules such as cyanide or nitric oxide may involve polar effects, where dipole–dipole or hydrogen-bonding interactions between a formally δ^- coordinated dioxygen and δ^+ amide hydrogen might retard dissociation of O_2 and hence raise the observed binding constant. A lively discussion continues in the literature between proponents of the distal-side steric model[8] and adherents of models based on polar effects.[9]

This research group has developed a family of totally synthetic non-porphyrin macrocyclic complexes, which model several pertinent features of natural hemoprotein systems.[10] This class of lacunar cyclidene complexes (structure I) contains peripheral substituents which define a cavity above one face of the macrocycle and hence restricts access to this axial site by a potential ligand.

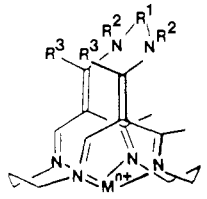

I

The R^1 and R^2 substituents are readily varied to adjust the dimensions of the cavity and the electron density at the metal site, which in turn provides a method of fine tuning the binding constant at this axial position. Variations of over 10^5 in the value of the equilibrium constant for dioxygen adduct formation,[11] and of the same magnitude for CO binding,[12,13] have been generated by alterations in R^1. For example, this group can be varied from the fairly flexible $-(CH_2)_6-$ bridge to the much tighter $-(CH_2)_4-$ unit.

The results of two structural studies have shown how the length of the polymethylene bridge affects the strength of binding of small molecules. An x-ray structure determination on an iron carbonyl adduct[12,13] in which $R^1 = -(CH_2)_5-$ shows a significant distortion of the bound CO, which is bent at both the iron and carbon atom centers. The Fe–C–O angle is 170.6 (5)°, and the Fe–C vector is displaced appreciably from the normal to the N_4 equatorial plane. In addition the central carbon of the pentamethylene bridge moves as far away as possible from the carbonyl ligand. Similarly, distortion of an isothiocyanate bound to a cobalt(III) center has also been observed.[14,15] In $[Co\{(CH_2)_6(MeNEthi)_2[16]tetraeneN_4\}(NCS)_2]Cl$ the NCS ligand coordinated within the lacuna is distorted to a much greater extent than that bound at the open axial position; the Co–N–C angles are 148.5 and 172.3°, respectively. The present communication is an extension of these studies, in which the cobalt(III) complex with the cyclidene ligands having $R^1 = -(CH_2)_5-$ and $-(CH_2)_7-$ have been synthesized as the hexafluorophosphate salts of their bis(isothiocyanato) complexes. The pentamethylene-bridged complex has been subjected to an x-ray structure determination. In this complex one of the NCS groups is found to be even more severely distorted than in the corresponding hexamethylene-bridged derivative. The implications of this structural deformation are discussed.

Experimental Section

Materials. Solvents and reagents used in the synthesis of the cobalt(II) and cobalt(III) complexes were of reagent grade. Solvents were dried by using published procedures[16] and thoroughly degassed before use.

Synthesis. The synthesis of the bridged nickel(II) cyclidene complex I ($R^1 = -(CH_2)_5-$, $R^2 = R^3 = -CH_3$),[17,18] demetalation to produce the protonated ligand salt,[17] and insertion of cobalt(II)[14] have all been described before. The synthesis of the cobalt(II) complex was carried out inside a Vacuum Atmosphere glovebox under an atmosphere of dry nitrogen.

Bis(isothiocyanato)(2,3,9,10,12,18-hexamethyl-3,9,13,17,20,24-hexaazabicyclo[9.7.7]pentacosa-1,10,12,17,19,24-hexaene-κ^4N)cobalt(III) Hexafluorophosphate, $[Co\{(CH_2)_5(MeNEthi)_2[16]tetraeneN_4\}(NCS)_2](PF_6)$. One gram (1.3 mmol) of $[Co\{(CH_2)_5(MeNEthi)_2[16]tetraeneN_4\}](PF_6)_2$ was dissolved in 10 mL of acetonitrile. One gram (1.3 mmol) of sodium thiocyanate was dissolved in 25 mL of water, and the two solutions were mixed, with sufficient acetonitrile added to keep all materials in solution. To this mixture was added dropwise 0.7 g (1.3 mmol) of ammonium hexakis(nitrato)cerate(IV) dissolved in 10 mL of methanol. The reaction mixture was filtered and removed from the drybox and was allowed to concentrate at room temperature. After about 2 weeks, the dark red crystalline product was isolated and redissolved in a minimum amount of acetonitrile. A saturated solution of NH_4PF_6 (ca. 1.5 g) in ethanol was added dropwise until the solution just became cloudy. This mixture was allowed to stand at room temperature for an additional week, after which period the deep red crystalline product was isolated by filtration and dried in vacuo.

Bis(isothiocyanato)(2,3,10,11,13,19-hexamethyl-3,10,14,18,21,25-hexaazabicyclo[10.7.7]hexacosa-1,11,13,18,20,25-hexaene-κ^4N)cobalt(III) Hexafluorophosphate, $[Co\{(CH_2)_6(MeNEthi)_2[16]tetraeneN_4\}(NCS)_2](PF_6)$. One gram (1.3 mmol) of $[Co\{(CH_2)_6(MeNEthi)_2[16]tetraeneN_4\}](PF_6)_2$ was dissolved in 50 mL of acetonitrile. One gram (13 mmol) of sodium thiocyanate, dissolved in 25 mL of water, was added. To this mixture was added dropwise 0.7 g (1.3 mmol) of ammonium hexakis(nitrato)cerate(IV), dissolved in 10 mL of methanol. The solution darkened in color and was filtered and removed from the drybox. After concentration for about 1 week under ambient conditions, the crystals that had formed were collected by filtration, washed with methanol, and dried in vacuo.

Bis(isothiocyanato)(2,11-diphenyl-3,10,13,19-tetramethyl-3,10,14,18,21,25-hexaazabicyclo[10.7.7]hexacosa-1,11,13,18,20,25-hexaene-κ^4N)cobalt(III) Hexafluorophosphate, $[Co\{(CH_2)_6(BzNMe)_2[16]tetraeneN_4\}(NCS)_2](PF_6)$, Bis(isothiocyanato)(2,3,11,12,14,20-hexamethyl-3,11,15,19,22,26-hexaazabicyclo[11.7.7]heptacosa-1,12,14,19,21,26-hexaene-κ^4N)cobalt(III) Hexafluorophosphate, $[Co\{(CH_2)_7(MeNEthi)_2[16]tetraeneN_4\}(NCS)_2](PF_6)$, and Bis(isothiocyanato)(2,12-dimethyl-3,11-bis[1-(dimethylamino)ethylidene]-1,5,9,13-tetraazacyclohexadeca-1,4,9,12-tetraene-κ^4N)cobalt(III) Hexafluorophosphate, $[Co\{(CH_3)_2(MeNEthi)_2[16]tetraeneN_4\}(NCS)_2](PF_6)$. These compounds were synthesized by the same procedure used for $[Co\{(CH_2)_5(MeNEthi)_2[16]tetraeneN_4\}(NCS)_2](PF_6)_2$, with the difference that the red crystals originally obtained from the acetonitrile/water/methanol mixture were recrystallized from acetone/water without the addition of excess NH_4PF_6. Yields and analytical data for the new compounds are shown in Table I.

(4) Collman, J. P.; Brauman, J. I.; Doxsee, K. M.; Halbert, T. R.; Hayes, S. E.; Suslick, K. S. *J. Am. Chem. Soc.* **1978**, *100*, 2761.
(5) Almog, J.; Baldwin, J. E.; Huff, J. *J. Am. Chem. Soc.* **1975**, *97*, 227.
(6) Momenteau, M.; Loock, B.; Mispelter, J.; Bisagni, E. *Nouv. J. Chim.* **1979**, *3*, 77.
(7) Diekmann, H.; Chang, C. K.; Traylor, T. G. *J. Am. Chem. Soc.* **1971**, *93*, 4068.
(8) Collman, J. P.; Brauman, J. I.; Iverson, B. L.; Sessler, J. L.; Morris, R. M.; Gibson, Q. H. *J. Am. Chem. Soc.* **1983**, *105*, 3052.
(9) (a) Traylor, T. G.; Koga, N.; Deardurff, L. A. *J. Am. Chem. Soc.* **1985**, *107*, 6504. (b) Mispelter, J.; Momenteau, M.; Lavalette, D.; Lhoste, J. M. *J. Am. Chem. Soc.* **1983**, *105*, 5165.
(10) Busch, D. H.; Cairns, C. *Prog. Macrocyclic Chem.* in press, and references therein.
(11) Stevens, J. C.; Busch, D. H. *J. Am. Chem. Soc.* **1980**, *102*, 3285.
(12) Zimmer, L. L. Ph.D. Thesis, The Ohio State University, 1979.
(13) Busch, D. H.; Zimmer, L. L.; Grzybowski, J. J.; Olszanski, D. J.; Jackels, S. C.; Callahan, R. W.; Christoph, G. G. *Proc. Natl. Acad. Sci. U.S.A.* **1981**, *78*, 5919.
(14) Stevens, J. C.; Jackson, P. J.; Schammel, W. P.; Christoph, G. G.; Busch, D. H. *J. Am. Chem. Soc.* **1980**, *102*, 3283.
(15) Jackson, P. J. Ph.D. Thesis, The Ohio State University, 1981.
(16) Vogel, A. E. *A Textbook of Practical Organic Chemistry*, 3rd ed.; Wiley: New York, 1966; pp 163–179.
(17) Busch, D. H.; Olszanskli, D. J.; Stevens, J. C.; Schammel, W. P.; Kojima, M.; Herron, N.; Zimmer, L. L.; Holter, K. A.; Mocak, J. *J. Am. Chem. Soc.* **1981**, *103*, 1472.
(18) Korybut-Daszkiewicz, B.; Kojima, M.; Cameron, J. H.; Herron, N.; Chavan, M. Y.; Jircitano, A. J.; Coltrain, B. K.; Neer, G. L.; Alcock, N. W.; Busch, D. H. *Inorg. Chem.* **1984**, *23*, 903.

Table I. Analytical Data for New Cobalt(III) Cyclidene Complexes

R^1	R^2	R^3	yield, %	formula	anal.	% C	% H	% N	% S
$(CH_2)_5$	CH_3	CH_3	54	$CoC_{27}H_{42}N_8S_2PF_6$	calcd	43.43	5.67	15.01	8.60
					found	43.39	5.70	14.96	8.50
$(CH_2)_6$	CH_3	CH_3	65	$CoC_{28}H_{44}N_8S_2PF_6$	calcd	44.20	5.82	14.71	8.40
					found	44.35	5.90	14.80	8.66
$(CH_2)_6$	CH_3	C_6H_5	25	$CoC_{29}H_{46}N_8S_2PF_6$[a]	calcd	49.96	5.75	12.16	6.95
					found	49.42	5.50	12.03	6.51
$(CH_2)_7$	CH_3	CH_3	52	$CoC_{38}H_{48}N_8S_2PF_6$	calcd	44.90	6.00	14.48	8.29
					found	44.50	5.92	13.50	8.82
CH_3	CH_3	CH_3	68	$CoC_{24}H_{38}N_8S_2PF_6$	calcd	40.85	5.40	15.89	9.07
					found	40.64	5.74	15.53	8.64

[a] Analyzes as a dihydrate.

Table II. Summary of Crystallographic Data for $[Co\{(CH_2)_5(MeNEthi)_2[16]tetraeneN_4\}(NCS)_2](PF_6)$

mol wt	746.6
a, Å	10.342 (4)
b, Å	14.857 (4)
c, Å	21.933 (4)
V, Å^3	3370 (2)
T, K	290
Z	4
$F(000)$	1552
space group	$P2_12_12_1$ (D_2^4, No. 19)
d_{calcd}, g cm^{-3}	1.47
cryst dimens, mm	0.24 × 0.32 × 0.31
abs coeff (μ), cm^{-1}	7.60
radiation used	Mo Kα (λ(Mo Kα) = 0.71069 Å)
$2\theta_{max}$, deg	50
no. of unique data	3359
no. of data used in refinement, $[I/\sigma(I) > 3]$	2458
no. of atoms in asym unit	87
R_1	0.042
R_w[a]	0.047
data collcd	$+h,+k,\pm l$

[a] $R_w = [\sum w|\Delta F|^2/\sum|F_o|^2]^{1/2}$.

Crystal Data. The title complex crystallized as deep red pyramids from an acetonitrile/ethanol mixture. A crystal (dimensions 0.24 × 0.35 × 0.34 mm) was mounted for examination on a Syntex $P2_1$ four-circle automated diffractometer. The unit cell dimensions and their esd's were obtained from a least-squares fit to 15 high-angle reflections using Mo Kα radiation (λ = 0.71069 Å) at 290 K. Systematic absences $h00$ ($h \neq 2n$), $0k0$ ($k \neq 2n$), and $00l$ ($l \neq 2n$), indicated space group $P2_12_12_1$. Intensity data were collected by the ω–2θ technique with variable scan rate between 3 and 29° min^{-1}. The maximum 2θ was 50°, with scan range ±1.0° around the Kα_1–Kα_2 angles. Backgrounds were measured at each end of the scan for 0.25 of the scan time. Three standard reflections were monitored every 200 reflections and showed slight changes during data collection; data were rescaled to correct for this. A total of 3359 reflections, of which 2458 had $I/\sigma(I) > 3.0$, were collected and used in the structure determination. The reflections were corrected for Lorentz, polarization, and absorption effects, the last with ABSCOR;[19] maximum and minimum transmission factors were 0.89 and 0.87 respectively. Table II summarized the crystal characteristics and x-ray methodology used in the determination.

Solution and Refinement of the Structure. The structure was solved by the heavy-atom Patterson technique and refined by using successive Fourier syntheses. Anisotropic factors were used for all non-hydrogen atoms; hydrogen atoms were given fixed isotropic temperature factors with U = 0.07 Å^2. Those defined by the molecular geometry were inserted at calculated positions and not refined; methyl groups were treated as rigid CH_3 units, with their orientation taken from the strongest H atom peaks on a difference Fourier syntheses. The hexafluorophosphate counterion was disordered about a C_4 axis, and four additional fluoride ions were used to attempt to compensate for this; the original four fluorides (F(1)–F(6)) and the four additional atoms (F(7)–F(10)) were given occupancies of 0.7 and 0.3, respectively. Despite this, the largest peaks on the final difference map were near the PF_6^- ion. The final refinement used cascaded least-squares methods. The weighting scheme used was of the form $w = 1/\sigma^2(F) + g(F^2)$ with g = 0.0005, and was shown to be satisfactory by a weight analysis. At convergence the largest positive and negative peaks on a final difference Fourier synthesis had a density of ca. 0.3 e/Å^3. Final R = 0.042, and R_w = 0.047.

Computations were carried out by using SHELXTL[20] on a Data General DG30 computer, apart from absorption corrections, which were determined on a Burroughs B6700 computer. Scattering and anomalous dispersion factors were taken from ref 21. Final atom coordinates are

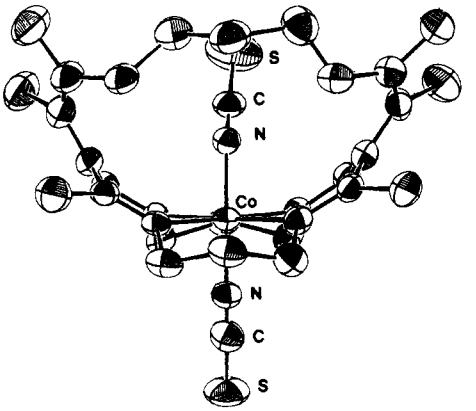

Figure 1. ORTEP drawing, looking into the cavity, for the complex $[Co^{III}L(NCS)_2]PF_6$, where L has the structure shown in structure I: $R^1 = -(CH_2)_5-$, $R^2 = R^3 = CH_3$.

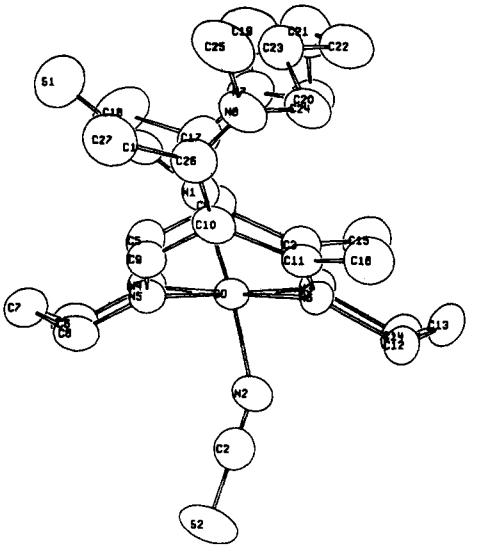

Figure 2. Side view of $[Co^{III}L(NCS)_2]PF_6$ showing distortion in both internal and external NCS groups. The atom-numbering scheme for the structure is also shown.

(19) Alcock, N. W. In *Crystallographic Computing*; Ahmed, F. R., Ed.; Mundsgaard: Copenhagen, 1970; p 271.

(20) Sheldrick, G. M. *SHELXTL User Manual*; Nicolet Instrument Co.: Madison, WI, 1983.

(21) *International Tables for X-ray Crystallography*; Kynoch: Birmingham, England, 1974; Vol. IV.

Table III. Atomic Coordinates (×10⁴) for the Non-Hydrogen Atoms of the Title Complex

atom	*x*	*y*	*z*	*U*, Å²
Co	3853 (1)	3984 (1)	5854 (1)	27 (1)
S(1)	7165 (2)	5732 (1)	5334 (1)	86 (1)
S(2)	2919 (2)	971 (1)	5986 (1)	67 (1)
P	9187 (2)	2308 (1)	7265 (1)	54 (1)
F(1)	9164 (5)	2817 (4)	6680 (2)	127 (3)
F(2)	9190 (7)	1709 (5)	7825 (3)	198 (4)
F(3)	8340 (9)	1652 (5)	6855 (4)	134 (4)
F(4)	10177 (9)	2914 (6)	7572 (3)	134 (4)
F(5)	7959 (9)	2712 (7)	7522 (5)	179 (5)
F(6)	10390 (9)	1914 (6)	6876 (4)	132 (4)
F(7)	9018 (17)	3313 (11)	7472 (7)	91 (5)
F(8)	10604 (15)	2358 (10)	7449 (7)	81 (5)
F(9)	9372 (17)	1289 (11)	7178 (7)	96 (6)
F(10)	7738 (13)	2192 (9)	7225 (6)	53 (4)
N(1)	4781 (4)	5095 (3)	5698 (2)	31 (1)
N(2)	3069 (4)	2843 (3)	5984 (2)	35 (2)
N(3)	3307 (4)	4405 (3)	6659 (2)	34 (1)
N(4)	5429 (4)	3556 (3)	6241 (2)	32 (1)
N(5)	4402 (4)	3605 (3)	5049 (2)	29 (1)
N(6)	2289 (4)	4463 (3)	5463 (2)	29 (1)
N(7)	5810 (5)	6396 (3)	7131 (2)	45 (2)
N(8)	3583 (5)	6515 (3)	4378 (2)	46 (2)
C(1)	5772 (6)	5346 (3)	5544 (3)	38 (2)
C(2)	3002 (6)	2055 (4)	5991 (3)	43 (2)
C(3)	4094 (6)	4803 (4)	7033 (2)	33 (2)
C(4)	5478 (6)	4831 (4)	6915 (2)	36 (2)
C(5)	6030 (5)	4055 (4)	6629 (2)	36 (2)
C(6)	6066 (6)	2721 (4)	6026 (2)	43 (2)
C(7)	6328 (6)	2745 (4)	5358 (2)	42 (2)
C(8)	5131 (6)	2765 (4)	4959 (3)	38 (2)
C(9)	4262 (5)	4127 (3)	4590 (2)	33 (2)
C(10)	3495 (6)	4932 (3)	4585 (2)	36 (2)
C(11)	2316 (5)	4917 (4)	4956 (3)	34 (2)
C(12)	1041 (5)	4298 (4)	5777 (3)	41 (2)
C(13)	1025 (6)	4707 (4)	6403 (3)	46 (2)
C(14)	1954 (5)	4250 (4)	6836 (3)	45 (2)
C(15)	3681 (7)	5131 (4)	7659 (3)	49 (2)
C(16)	1131 (7)	5329 (4)	4682 (3)	55 (2)
C(17)	6262 (6)	5553 (4)	7113 (2)	39 (2)
C(18)	7663 (6)	5407 (5)	7269 (4)	66 (3)
C(19)	6458 (8)	7099 (4)	7480 (3)	62 (3)
C(20)	4636 (6)	6690 (4)	6813 (3)	47 (2)
C(21)	4812 (7)	7557 (5)	6443 (3)	62 (3)
C(22)	3753 (7)	7664 (4)	5964 (3)	61 (3)
C(23)	4181 (6)	7382 (4)	5326 (3)	51 (2)
C(24)	3167 (6)	6826 (4)	4993 (3)	46 (2)
C(25)	3924 (10)	7274 (4)	3969 (3)	72 (3)
C(26)	3887 (6)	5662 (4)	4244 (2)	43 (2)
C(27)	4771 (8)	5533 (5)	3693 (3)	62 (3)

given in Table III, and bond lengths and angles in Table IV.

Discussion

X-ray Crystal Structure. Figure 1 shows an ORTEP drawing of the title complex, looking into the lacuna defined by the R^1 and R^2 peripheral substituents, and shows that the pentamethylene bridge is sufficiently flexible and the cavity sufficiently large to allow coordination at the internal axial site.

The side view (Figure 2) is remarkable; it shows clearly that the internal isothiocyanate is severely distorted, being bent away from the normal to the equatorial N_4 plane by just over 39° (the Co–N(1)–C(1) angle is 140.84°). The numbering scheme is shown in Figure 2. In addition the isothiocyanate bends at the metal site, with the Co–N(1) bond tilted at about 5° from the perpendicular to the equatorial plane defined by the four nitrogens. This behavior has been previously noted for the iron carbonyl adduct with the same bridge length (R^2 = H).[13] This weakened bonding is manifested in the Co–N(1) bond length which, at 1.940 Å, is 0.04 Å longer than the external Co–N(2) bond. Interestingly, the difference in axial coordinate bond strengths is not reflected in the two C–S bond lengths, which are essentially identical.

These structural features parallel those previously observed[14] for the hexamethylene-bridged cobalt(III) complex, with the most notable difference being in the distortion of the external isothiocyanate that is coordinated at the open axial site. In the hexamethylene-bridged case, the external cobalt–isothiocyanate linkage approached linearity (Co–N(2)–C(2) = 172.3°), while in the present case the analogous angle is 156.6 (5)°.

The reason for the marked difference becomes clear upon inspection of the packing diagram of the latter complex, shown in Figure 3. In this diagram, viewed down the *a* and *c* axes, one can see that the packing of the plate-like cations (see the *c* projection) leaves relatively little space for the PF_6^- group. The counterion occupies a modest space between, but in the same plane as, the cations (see the *a* projection). This is presumably the best available space but carries the penalty of a very close approach between F(6) and S(2). This interaction is indicated by the dotted lines in Figure 3. To relieve this crowding, the NCS group bends by ca. 23°. (For a linear NCS the S(2)–F(6) contact would be

Table IV. Bond Distances (Å) and Angles (deg) with Their Estimated Standard Deviations for the Title Complex

A. Bond Distances

Co–N(1)	1.940 (4)	Co–N(2)	1.900 (4)
Co–N(3)	1.955 (4)	Co–N(4)	1.944 (4)
Co–N(5)	1.940 (4)	Co–N(6)	1.965 (4)
S(1)–C(1)	1.617 (6)	S(2)–C(2)	1.613 (6)
N(2)–C(2)	1.173 (7)	N(1)–C(1)	1.142 (7)
N(3)–C(14)	1.471 (7)	N(3)–C(3)	1.299 (7)
N(4)–C(6)	1.481 (7)	N(4)–C(5)	1.289 (7)
N(5)–C(9)	1.280 (7)	N(5)–C(8)	1.471 (7)
N(6)–C(12)	1.483 (7)	N(6)–C(11)	1.300 (7)
N(7)–C(19)	1.457 (8)	N(7)–C(17)	1.338 (7)
N(8)–C(24)	1.489 (7)	N(7)–C(20)	1.468 (8)
N(8)–C(26)	1.339 (7)	N(8)–C(25)	1.484 (8)
C(3)–C(15)	1.517 (8)	C(3)–C(4)	1.455 (8)
C(4)–C(17)	1.413 (8)	C(4)–C(5)	1.431 (8)
C(7)–C(8)	1.516 (8)	C(6)–C(7)	1.491 (7)
C(10)–C(11)	1.467 (8)	C(9)–C(10)	1.434 (7)
C(11)–C(16)	1.496 (9)	C(10)–C(26)	1.378 (8)
C(13)–C(14)	1.513 (8)	C(12)–C(13)	1.501 (8)
C(20)–C(21)	1.532 (9)	C(17)–C(18)	1.505 (9)
C(22)–C(23)	1.528 (9)	C(21)–C(22)	1.526 (10)
C(26)–C(27)	1.528 (9)	C(23)–C(24)	1.521 (9)

B. Bond Angles

N(1)–Co–N(2)	175.1 (2)	N(1)–Co–N(3)	91.7 (2)
N(2)–Co–N(3)	91.6 (2)	N(1)–Co–N(4)	86.6 (2)
N(2)–Co–N(4)	90.0 (2)	N(3)–Co–N(4)	87.3 (2)
N(1)–Co–N(5)	86.6 (2)	N(2)–Co–N(5)	90.1 (2)
N(3)–Co–N(5)	178.2 (2)	N(4)–Co–N(5)	93.2 (2)
N(1)–Co–N(6)	91.3 (2)	N(2)–Co–N(6)	92.1 (2)
N(3)–Co–N(6)	92.4 (2)	N(4)–Co–N(6)	177.8 (2)
N(5)–Co–N(6)	87.0 (2)	Co–N(2)–C(2)	156.6 (5)
Co–N(1)–C(1)	140.8 (4)	Co–N(3)–C(14)	117.6 (3)
Co–N(3)–C(3)	122.4 (4)	Co–N(4)–C(5)	120.3 (4)
C(3)–N(3)–C(14)	120.0 (5)	C(5)–N(4)–C(6)	118.5 (5)
Co–N(4)–C(6)	120.6 (3)	Co–N(5)–C(9)	120.5 (4)
Co–N(5)–C(8)	121.2 (3)	Co–N(6)–C(11)	122.9 (4)
C(8)–N(5)–C(9)	117.9 (4)	C(11)–N(6)–C(12)	120.1 (4)
Co–N(6)–C(12)	116.9 (3)	C(17)–N(7)–C(20)	123.6 (5)
C(17)–N(7)–C(19)	121.7 (5)	C(24)–N(8)–C(25)	112.4 (4)
C(19)–N(7)–C(20)	114.6 (5)	C(25)–N(8)–C(26)	122.0 (5)
C(24)–N(8)–C(26)	124.1 (5)	S(2)–C(2)–N(2)	178.8 (6)
S(1)–C(1)–N(1)	178.3 (5)	N(3)–C(3)–C(15)	122.8 (5)
N(3)–C(3)–C(4)	121.1 (5)	C(3)–C(4)–C(5)	116.6 (5)
C(4)–C(3)–C(15)	115.4 (5)	C(5)–C(4)–C(17)	121.1 (5)
C(3)–C(4)–C(17)	122.1 (5)	N(4)–C(6)–C(7)	111.9 (4)
N(4)–C(5)–C(4)	124.1 (5)	N(5)–C(8)–C(7)	111.0 (4)
C(6)–C(7)–C(8)	114.8 (5)	C(9)–C(10)–C(11)	116.3 (5)
N(5)–C(9)–C(10)	125.0 (5)	C(11)–C(10)–C(26)	123.9 (5)
C(9)–C(10)–C(26)	119.9 (5)	N(6)–C(11)–C(16)	122.5 (5)
N(6)–C(11)–C(10)	120.0 (5)	N(6)–C(12)–C(13)	111.6 (4)
C(10)–C(11)–C(16)	116.9 (5)	N(3)–C(14)–C(13)	111.6 (5)
C(12)–C(13)–C(14)	112.7 (5)	N(7)–C(17)–C(18)	117.7 (5)
N(7)–C(17)–C(4)	121.3 (5)	N(7)–C(20)–C(21)	113.8 (5)
C(4)–C(17)–C(18)	120.9 (5)	C(21)–C(22)–C(23)	113.2 (6)
C(20)–C(21)–C(22)	111.5 (5)	N(8)–C(24)–C(23)	113.8 (5)
C(22)–C(23)–C(24)	112.9 (5)	N(8)–C(26)–C(27)	115.7 (5)
N(8)–C(26)–C(10)	123.9 (5)		
C(10)–C(26)–C(27)	120.4 (5)		

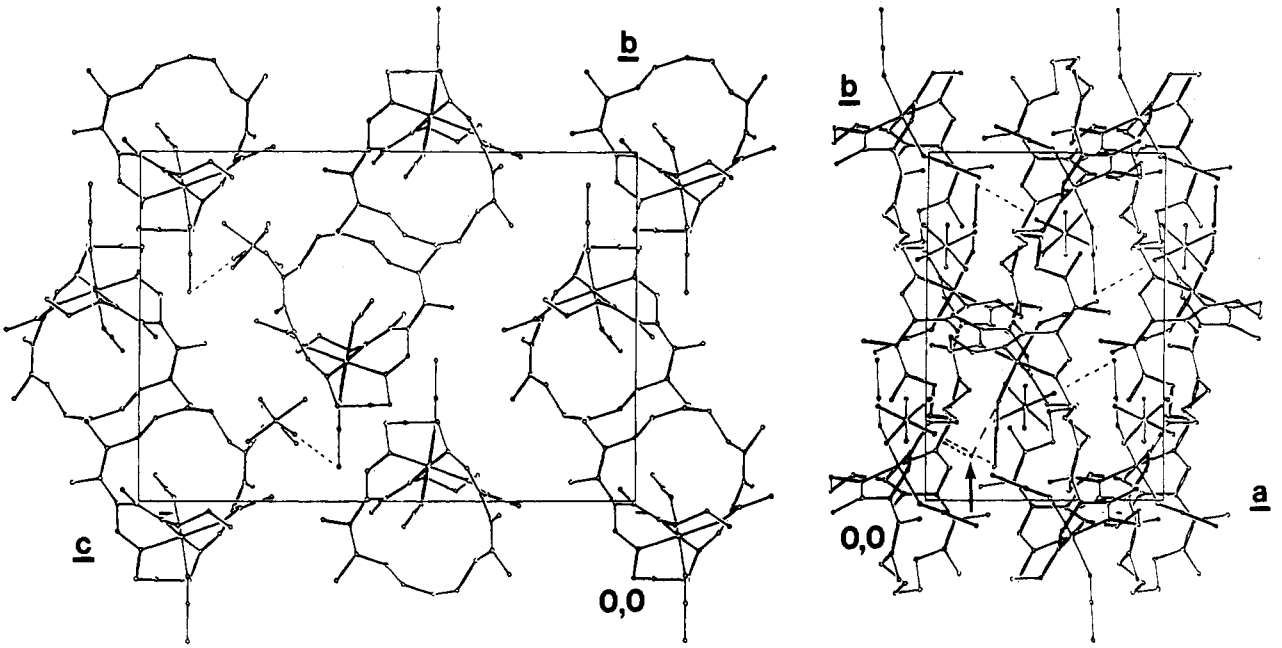

Figure 3. Crystal packing diagram of I ($R^1 = -(CH_2)_5-$, $R^2 = R^3 = CH_3$) in the *a* and *c* projections. Close intermolecular contacts are shown by dotted lines, with the contact to a hypothetical linear -NCS group arrowed.

Table V. Comparison of Structural Parameters for the Two Lacunar Cyclidene Bis(isothiocyanato)cobalt(III) Complexes with Structure I ($R^2 = R^3 = CH_3$)

	dist, Å						angle, deg	
R^1	Co–N(1)	Co–N(2)	N(1)–C(1)	C(1)–S(1)	N(2)–C(2)	C(2)–S(2)	Co–N(1)–C(1)	Co–N(2)–C(2)
$-(CH_2)_5-$	1.940 (4)	1.900 (4)	1.142 (7)	1.617 (6)	1.173 (7)	1.613 (6)	140.8 (4)	156.6 (5)
$-(CH_2)_6-$	1.94 (1)	1.88 (1)	1.17 (1)	1.60 (1)	1.17 (1)	1.60 (1)	148.5 (5)	172.3 (11)

2.36 Å; this is increased to 3.55 Å in the actual structure.) The counterion in the complex where $R^1 = -(CH_2)_6-$ is a chloride, which, because of its smaller size, is presumably able to fit easily into the lattice without causing undue interactions with any part of the cation.

The distortion of the internal isothiocyanate ligand can be attributed to van der Waals interactions with atoms of the pentamethylene bridge. Figure 4 shows some of the more important contacts. Much of the structure has been removed so the distances of interest can be emphasized. The closest contacts involve the nitrogen atom of the axial ligand with hydrogens on the terminal carbon atoms of the bridge (C(20) and C(24)), and these are probably largely responsible for the 5° tilt imposed on the Co–N(1) bond. Both the isothiocyanate carbon and sulfur atoms contact hydrogens on C(20) and C(23). The result of all of these interactions is to tilt the C–N–Co angle to 140.8° (from the expected 180°). The internal isothiocyanate ligand lies slightly closer to the side of the lacuna containing C(23) and C(24), a deviation that must reflect crystal-packing effects.

The remainder of the structure is unremarkable. As expected, the saturated portion of the equatorial girdle adopts chair conformations to minimize nonbonding contacts with the external isothiocyanate. All other bond lengths and angles are comparable with those observed in the hexamethylene-bridged molecule, although in the latter complex the two central carbon atoms of the bridge were disordered, leading to a less well-defined lacuna than in the present case. The only disorder observed in this species involves the PF_6^- ion, which is disordered about a C_4 axis; this does not, however, invalidate any of the steric arguments that have been used to explain the unusual conformation of the external isothiocyanate in the molecule.

Factors Influencing Isothiocyanate Coordination. The preceding discussion has shown the effects of two different sterically confined environments on the Co–N–C bond angle for an NCS ligand. Table V draws together the structural data that describe the sources of the distortion for both $R^1 = -(CH_3)_5-$ and $-(CH_2)_6-$.

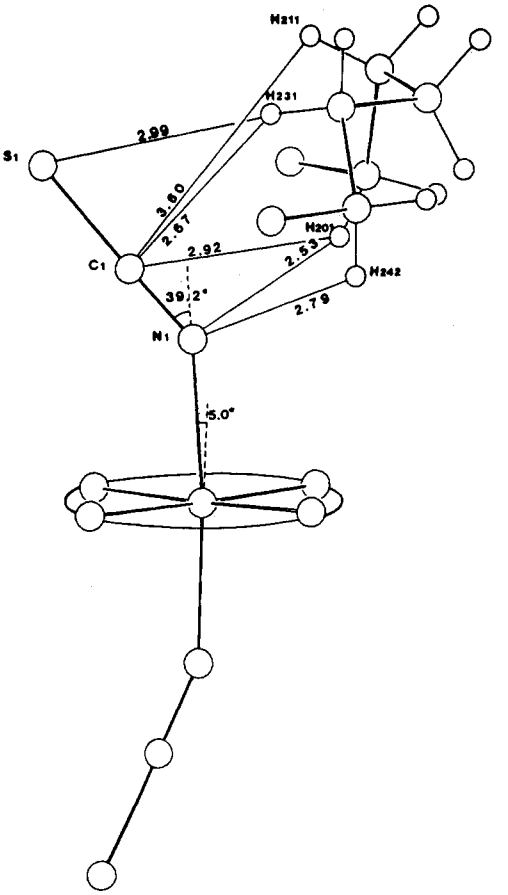

Figure 4. van der Waals contacts between the internal isothiocyanate ligand and hydrogen atoms on the polymethylene bridge. For clarity, only the atoms involved in the interactions have been included.

In theory there are three factors that can influence the extent of the distortion of an N-bonded thiocyanate. Each of these will now be considered briefly.

(i) Electronic Effects. As has been discussed before,[22-24] two resonance forms, II and III, can be written for an N-bonded thiocyanate ligand. The linear form (II) will be stabilized when

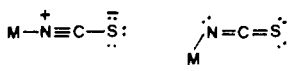

II III

the metal atom has d_π electrons available for back-bonding to the ligand. In the low-spin bis(isothiocyanato)iron(II) complexes described by Drew et at.,[24] all of the d electrons are involved in back-bonding to the tris(imine) portion of the equatorial macrocycle, and resonance form III was stabilized as a result. In the present cyclidene cobalt(III) complexes this situation is not realized; the d_{xz} and d_{yz} orbitals of the metal atom are potentially available for π-interaction with the orbitals of the thiocyanate ligand.

(ii) Intermolecular Steric Effects. Perhaps the clearest example of an isothiocyanate being bent as a result of intermolecular van der Waals interactions is shown by the complex dimethylbis(isothiocyanato)(terpyridyl) tin(IV).[25] The packing diagram reveals several close contacts between one NCS and an aromatic ring of a terpyridyl ligand on a neighboring molecule. The two Sn–N–C angles of 177.3 and 155.3° attest to the significance of this influence. In the present cyclidene complex, the presence of the PF_6^- counterion is seen to cause a similar effect on the NCS(2) ligand.

(iii) Intramolecular Steric Effects. This factor, a discussion of which forms the basis for this communication, has also been observed in other macrocyclic systems. Again the results of Drew and Nelson on pentadentate Schiff base complexes are instructive. In a bis(isothiocyanato)manganese(II) complex,[26] the nonplanarity of the macrocycle leads to significant crowding of one of the two axial NCS ligands. Consequently, this NCS(2) is more weakly bound (Mn–N(1) = 2.174 Å, while Mn–N(2)–C(2) = 135° vs. 150.9° for Mn–N(1)–C(1)). A similar situation exists in the cyclidene complex under discussion. Table IV indicates that NCS(1) is more weakly bound than NCS(2), as well as exhibiting a significantly more distorted bond angle, even after the effect of the intermolecular interaction is taken into account. The difference in Co–N bond lengths (0.04 Å) might be even more pronounced if one were comparing complexes with the same counterion.

In summary, the structural parameters in Table V, taken as a whole, do not allow an unequivocal explanation of the nonlinearity of the external isothiocyanate axial ligand. An electronic explanation is not entirely satisfactory. A correlation between the N–C bond length decreases and the N–C bond length increases with a decreasing M–N–C angle.[22] Our data on the two lacunar complexes do not obey this correlation, which was drawn from a rather limited data set. In addition, in both complexes the N–C and C–S bond lengths are in the range expected for triple and double bonds respectively. This fits neither resonance form II nor III and suggests that a steric explanation is more reasonable. While the steric argument for the internal isothiocyanato ligand is clear-cut, that for the other ligand is more open to debate. The M–N–C angle in coordinated isothiocyanates generally lies between 150 and 180°, and in many of the cases where it is toward the lower end of this range, the influence of steric effects is not obvious. We can, nevertheless, state that the angle of 156.6 (5)° in the present complex can be *reasonably* explained by interaction with a nearby hexafluorophosphate ion. We are, unfortunately, hampered by the presence of two different counterions in the two lacunar complex, which makes a direct comparison problematic. The data on the $(CH_2)_6$-bridged complex shows that other crystal packing effects can change the M–N–C angle (by 7.7° in that case).

Table VI. Selected IR Data for New Cobalt(III) Cyclidene Complexes[a]

R^1	R^2	R^3	$\nu_{C\equiv N}$, cm^{-1}	$\nu_{C=N}$, cm^{-1}
$(CH_2)_5$	CH_3	CH_3	2110, 2045	1620
$(CH_2)_6$	CH_3	CH_3	2100, 2050	1620
$(CH_2)_6$	CH_3	C_6H_5	2105, 2046	1620
$(CH_2)_7$	CH_3	CH_3	2102, 2032	1620
CH_3	CH_3	CH_3	2100	1640

[a] Hexafluorophosphate salts; measured in CH_3CN.

The infrared spectra of a series of these bis(isothiocyanato)cobalt(III) cyclidene complexes corroborates these conclusions (Table VI). Complexes with R^1 varying between $-(CH_2)_5-$ and $-(CH_2)_7-$ show two C≡N stretches at ca. 2105 and 2045 cm^{-1}, while an unbridged complex ($R^1 = -(CH_3)_2-$) shows a single resonance at 2100 cm^{-1},[15] as would be expected for a complex providing virtually no hindrance to six-coordination at the metal center. It is worth noting that several attempts to make the $(CH_2)_4$-bridged complex were unsuccessful. This result suggests that the lacuna in the pentamethylene-bridged complex is only barely spacious enough to accommodate an isothiocyanate ligand, as well as indicating that the cobalt(III) ion much prefers a six-coordinate environment. This latter point has been explored in some detail by electrochemical studies on the lacunar cobalt(II) cyclidene complexes.[27,28]

Conclusions

The structural characterization of a bis(isothiocyanato)cobalt(III) lacunar cyclidene complex extends our understanding of the effects of a "distal" bridge on the coordination properties of this family of synthetic hemoprotein models. This information has been used to design new complexes with optimal selectivity toward dioxygen vs. larger ligands, while at the same time preventing, in large measure, irreversible autoxidiation of the metal–dioxygen adduct once it is formed. The present study serves as a reminder that various kinds of steric and electronic factors should be considered in the design of model systems with prescribed properties. The lacunar family described here possesses the extremely useful property that peripheral structural modifications can be made that effect, in a controllable manner, the topology of the molecule and the electronic properties of the central metal atom. This has allowed a detailed study of the solution properties of these molecules, in particular the cobalt(II) and iron(II) complexes, since the coordination environment can be strictly controlled even under these conditions. Further studies will focus on approaches to modeling distal polar, as well as steric effects, by appropriate modification of the R^1 substituent.

Acknowledgment. The support of the National Science Foundation and National Institutes of Health is gratefully acknowledged.

Registry No. [Co{$(CH_2)_5$(MeNEthi)$_2$[16]tetraeneN$_4$}(NCS)$_2$](PF_6), 103933-45-5; [Co{$(CH_2)_6$(MeNEthi)$_2$[16]tetraeneN$_4$}(NCS)$_2$](PF_6), 103933-47-7; [Co{$(CH_2)_6$(BzNMe)$_2$[16]tetraeneN$_4$}(NCS)$_2$](PF_6), 103933-49-9; [Co{$(CH_2)_7$(MeNEthi)$_2$[16]tetraeneN$_4$}(NCS)$_2$](PF_6), 103933-51-3; [Co{$(CH_3)_2$(MeNEthi)$_2$[16]tetraeneN$_4$}(NCS)$_2$](PF_6), 103933-53-5; [Co{$(CH_2)_5$(MeNEthi)$_2$[16]tetraeneN$_4$}](PF_6)$_2$, 103958-62-9; [Co{$(CH_2)_6$(MeNEthi)$_2$[16]tetraeneN$_4$}](PF_6)$_2$, 103933-54-6.

Supplementary Material Available: Tables of anisotropic thermal parameters for all non-hydrogen atoms, hydrogen atom coordinates and associated isotropic thermal parameters, and structural features of the PF_6^- counterion (4 pages); tables of observed and calculated structure factors (15 pages). Ordering information is given on any current masthead page.

(22) Hazell, A. C. *J. Chem. Soc.* **1963**, 5745.
(23) Knox, J. R.; Eriks, K. *Inorg. Chem.* **1968**, *7*, 84.
(24) Drew, M. G. B.; bin Othman, A. H.; Nelson, S. M. *J. Chem. Soc., Dalton Trans.* **1976**, 1394.
(25) Naik, D. V.; Scheidt, W. R. *Inorg. Chem.* **1973**, *12*, 272.
(26) Drew, M. G. B.; bin Othman, A. H.; McFall, S. G.; McIlroy, P. D. A.; Nelson, S. M. *J. Chem. Soc., Dalton Trans.* **1977**, 438.
(27) Chavan, M. Y.; Ph.D. Thesis, The Ohio State University, 1983.
(28) Chavan, M. Y.; Meade, T. J.; Busch, D. H.; Kuwana, T. *Inorg. Chem.* **1986**, *25*, 314.